Daifuku *et al.*
Translational Medicine Communications (2024) 9:2
https://doi.org/10.1186/s41231-024-00161-3

Translational Medicine Communications

RESEARCH

Open Access

iMN041 is an immunotherapeutic and an effective treatment in mouse xenograft models of pancreatic cancer, renal cancer and triple negative breast cancer

Richard Daifuku[1*], Yu Zhang[2], Jingjing Wang[2] and Qingyang Gu[2]

Abstract

Background iMN013 (5-aza-2′,2′-difluorodeoxycytidine), a DNA methyl transferase inhibitor and ribonucleotide reductase inhibitor, and its prodrug iMN041 (3′,5′-di-trimethylsilyl-2′,2′-difluro-5- azadeoxycytidine), have been shown to be active in mouse xenograft models of hematogenous and solid tumors. In a xenograft of non-small cell lung cancer (NCI-H460), iMN041 treated mice demonstrated a marked inflammatory response upon analysis of tumor histology, which was hypothesized to be mediated by upregulation of natural killer (NK) cells. This study aimed to characterize the antitumor immune responses generated by iMN041 and test the efficacy iMN041 in solid tumors with poor prognosis.

Methods In the Renca syngeneic mouse model, tumors were harvested following two doses of iMN041 or vehicle control, and analyzed by fluorescent-activated cell sorting for an antitumor immune response. iMN041 was also tested for tumor growth inhibition and animal survival for up to 42 days in xenograft models of pancreatic, renal, and triple negative breast cancer.

Results Tumors from mice implanted with the Renca cell line and treated with iMN041 demonstrated an increase in granzyme B in NK ($p = 0.024$) and NKT cells ($p = 0.004$), an increase in the ratios of CD8-T to regulatory T cells (Treg) ($p = 0.0026$) and CD4-T to Treg cells ($p = 0.022$) and a decrease in myeloid-derived suppressor cells ($p = 0.040$), compared to vehicle controls. A significant decrease in MAGE-A positive tumor cells in treated mice, concordant with a proportional decrease in all live tumor cells, suggests that these cells are one of the main targets of the activated immune system. Xenograft models of the triple negative breast cancer cell line DU4475, renal cancer cell lines 786-O and Caki-1, and pancreatic cancer cell lines CFPAC-1 and SW1990, demonstrated significantly lower tumor volumes, and, where there were a sufficient number of events, significantly improved survival in treated mice compared to vehicle control mice.

Conclusions In mouse cancer models, iMN041 is an effective treatment for solid tumors mediated in part through a unique antitumor immune response.

Keywords Cancer, Breast, Pancreatic, Renal, Immunotherapy, DNA methyltransferase, Ribonucleotide reductase, MAGE

*Correspondence:
Richard Daifuku
Richard@epigeneticspharma.com
Full list of author information is available at the end of the article

Background

iMN013 (5-aza-2',2'-difluorodeoxycytidine, previously NUC013) is a DNA methyl transferase inhibitor (DNMTI) and a ribonucleotide reductase inhibitor (RNRI). In vitro, iMN013 demonstrated activity against one or more cell lines in all nine tumor tissues in the NCI60 panel, including breast, colon, central nervous system, renal, lung, melanoma, ovarian, prostate and hematogenous tissues. In leukemic cell lines, iMN013 induced morphological changes that were suggestive of cell differentiation and lead to cell apoptosis. Subsequently, iMN013 was shown to be an effective treatment in mouse xenograft models of leukemia (HL-60) and colon cancer (LoVo) [1]. Because of the short half-life of IMN013, the prodrug, iMN041 (3',5'-di-trimethylsilyl-2',2'-difluro-5-azadeoxycytidine, previously NUC041), was synthesized and developed. A half-life of up to 3.4 hours was observed for iMN013 released from iMN041 in mice. In an animal model of non-small cell lung cancer (NCI-H460), the administration of IMN041 led to tumor regression. Based on tumor histology, it was hypothesized that part of the mechanism of action of iMN041 in nude mice was through upregulation of the immune system and, in particular, natural killer (NK) cells [2].

Following further refinement of the iMN041 formulation, the current study was initiated to demonstrate (1) the effect of iMN041 on the upregulation of the antitumor immune response in a syngeneic tumor mouse model and (2) the efficacy of iMN041 in mouse xenografts of human clear cell renal cell cancer (ccRCC), pancreatic cancer and triple negative breast cancer (TNBC).

Methods

Determination of half-maximal inhibitory concentation (IC50)

IC50 were determined for the following cell lines: : EMT-6 (RRID:CVCL_1923), 4T1 (RRID:CVCL_0125), DU4475 (RRID:CVCL_1183), MCF-7 (RRID:CVCL_0031), MDA-MB-231 (RRID:CVCL_0062), BxPC-3 (RRID:CVCL_0186), CFPAC-1 (RRID:CVCL_1119), MiaPaCa-2 (RRID:CVCL_0428), SW1990 (RRID:CVCL_1723) and Renca (RRID:CVCL_2174).

All cell lines were grown in RPMI 1640 medium supplemented with 10% fetal bovine serum (FBS), 0.1 mM non-essential amino acids, and 1 mM sodium pyruvate. iMN013 (10 mM) was solubilized in ice-cold phosphate-buffered saline (PBS) at pH 7.4 immediately prior to use. One 96 well plate for each cell line was seeded at 5,000 cells per well in a total volume of 50 µL per well and left overnight. The following day, cells were exposed to serial dilutions of IMN013 ranging from 100 µM to 0.1 µM. The drug exposed cells were incubated at 37°C for 72 hours (h).

In wells redosed every 12 h. After a 12 h incubation with the drug, all media were removed from the control wells and replaced with fresh media, whereas all media were removed from the treated wells and replaced with fresh media with the appropriate iMN013 concentration. For DU4475, because the cells grew in suspension, 1 µL of PBS or the requisite concentration of the study drug was added every 12 h to the medium.

At the end of the 72 h exposure period, the plates were removed for the CellTiter-Glo assay from an incubator at 37°C and 5% CO2, and placed on the bench at room temperature for 30 minutes (min). The CellTiter-Glo reagent (100 µL) was added, mixed for 2 min and incubated for 10 min at room temperature. Luminescence was recorded using a Synergy 4.0.

Formulation

The formulation for iMN041 (Latitude Pharmaceuticals, San Diego, CA, USA), was composed of soy lethicin (S-100), DSPE-PEG 2000 (9% weight/weight for FS-19 and 10% for FS-14), sesame oil and alcohol. These four constituents were placed in a vial and warmed to 40°C until all products were dissolved, and the vehicle was vortexed. Subsequently, the vehicle was filtered through a 0.22 µm syringe filter, iMN041 was added, and the formulated product was heated to 40°C, vortexed, and stored at -20°C.

Analytical method for iMN013

All blood samples were transferred to pre-chilled commercial EDTA-K2 tubes. Blood was transferred to an assay tube and IS6 in acetonitrile (ACN) was added to achieve a final ratio in blood internal standard of 6 in 1 in ACN (labetalol, tolbutamide, verapamil, dexamethasone, glyburide, and celecoxib 100 ng/mL for each at 1:10 (volume:volume)). The samples were centrifuged at 12,000 x g at 4°C for 15 min to separate the supernatant as soon as possible. Supernatant samples were collected and transferred into polypropylene tubes, quickly frozen on dry ice, and stored at -70±10°C until LC/MS/MS analysis.

Plasma concentration vs. time data were plotted and analyzed by non-compartmental approaches using the Phoenix WinNonlin 6.3 software program. Pharmacokinetic (PK) parameters were calculated according to the dosing route.

Fluorescent activated cell sorting (FACS) analysis

Tumor samples were processed into single cell suspensions containing mixed enzymes. Then cell suspension was applied to staining with Live/Dead (Biolegend-423106) and fluorophore-conjugated monoclonal antibodies of surface markers as following:

anti-CD45- (BioLegend Cat# 103111, RRID:AB_312976), anti-CD3-APC-Cy7 (BioLegend Cat# 100221, RRID: AB_2057374), anti-CD11b-AF532 (Thermo Fisher Scientific Cat# 58-0112-82, RRID:AB_2811905), anti-CD4-APC-Cy5.5 (Thermo Fisher Scientific Cat# MCD0419, RRID:AB_10375030), anti-CD8-Pacific Orange (Thermo Fisher Scientific Cat# MCD0830, RRID: AB_10376311), anti-CD25-BV650 (BioLegend Cat# 102037, RRID:AB_11125760), anti- CD49b-PE-Cy5 (Thermo Fisher Scientific Cat# 15-5971-82, RRID: AB_2573070), anti-Ly6C-BV785 (BioLegend Cat# 128041, RRID:AB_2565852), anti-Ly6G-PE-Dazzle594 (Bio-Legend Cat# 127647, RRID:AB_2566319), anti-F4/80-BB700 (BD Biosciences Cat# 746070, RRID:AB_ 2743450), anti-MHC class II- BV605 BD (Bio-sciences Cat# 563413, RRID:AB_2738190), anti-CD11c-AF488 (BioLegend Cat# 117313, RRID:AB_492849), anti-MHC class I-APC (BioLegend Cat# 114713, RRID: AB_2734173). After fixation and permeabilization (eBioscience-00-5523), following intracellular staining with antibodies: anti-FoxP3-PE- Cy7 (Thermo Fisher Scientific Cat# 25-5773-82, RRID:AB_891552), anti-CD206-AF700 (BioLegend Cat# 141733, RRID:AB_2629636), anti-GranzymeB-BV421 (BioLegend Cat# 396413, RRID:AB_2810602) and anti-MAGEA-PE (Santa Cruz Biotechnology Cat# sc-20033 PE, RRID:AB_2935836). The stained cells were washed twice with DPBS and suspended for fluorescence detection using a flow cytometer (Cytek- Aurora 3000). Isotypes for MAGE-A (Santa Cruz Biotechnology), and fluorescence-minus-one controls (FMO) for granzyme B were used for gating.

Animal tumor models

The following tumor cells lines were used in this series of experiments: Renca, 786-O (RRID:CVCL_1051), Caki-1 (RRID:CVCL_0234), SW1990, CFPAC-1, and DU4475. Tumor cells were maintained in RPMI-1640 medium supplemented with 10% FBS at 37°C in an atmosphere of 5% CO2. Cells in the exponential growth phase were harvested and counted for tumor inoculation. BALB/c nude, female (Zhejiang Vital River Laboratory Animal Technology Co., Ltd., Strain code: 409), weighing approximately 18-22 g, were used in these studies (n = 10/group), except for Renca studies which used BALB/c female mice (Zhejiang Vital River Laboratory Animal Technology Co., Ltd., Strain code: 211). Each mouse was inoculated subcutaneously (SC) in the right flank with tumor cells (5 X 10^6) in 200 µL PBS mixed with Matrigel (50:50) for tumor development. To ensure minimum variation in tumor size, typically 1.8-fold the number of animals were inoculated than were required for the study. The animals were randomized and treatment was initiated when the average tumor size reached the specified size for the study. Before commencement of treatment, all animals were weighed and tumor volumes were measured. As tumor volume can affect the effectiveness of any given treatment, mice were assigned to groups using a randomized block design based on their tumor volumes. This ensured that all groups were comparable at baseline. After inoculation, animals were monitored daily for morbidity and mortality. Mice administered > 0.6 mg iMN041 had their dose reduced to 0.6 mg if their weight loss was > 5% and < 10%. The treated mice had their dose held if the weight loss was > 10%. The study was terminated at 6 weeks, if the animals survived that period. Tumor sizes were measured twice per week in two dimensions using a caliper, and the volume was expressed in mm^3 using the formula: $V = 0.5\ a\ X\ b^2$ where a and b are the long and short diameters of the tumor, respectively.

In this study, an event was defined as animal death, body weight loss > 20%, or a tumor burden > 2 g. The latter two criteria were required by the animal-use protocol and animal welfare policy of WuXi App Tec and the animals were then euthanized.

Histology

Tumors from mice inoculated with Caki-1 were fixed in 10% neutral buffered formalin. The fixed neoplasm was trimmed, processed, embedded and microtomed (approximately 4 µm sections). Tissue sections were mounted on glass slides, stained with hematoxylin and eosin (H&E), and coverslipped. Slides were submitted to a veterinary pathologist for a histopathologic evaluation. HALO software was trained to classify regions of the tissue into active tumor and non-tumor components. Non tumor components included stroma and areas of tumor necrosis, and from these data the percentage of tumor necrosis was determined.

Statistical analysis

Power analysis: In xenograft models, n = 10/group will provide a 0.986 average power to detect a ratio of tumor volume in iMN041 treated animals to vehicle control animals of (T/C) below 0.4 [3].

Statistical analyses were performed using GraphPad Prism version 9.5.0. All p values were two-tailed.

All statistical analyses, except those mentioned below, were performed using an unpaired t-test, except for the comparison of Renca, 786-O and Caki-1 tumor volumes, where the starting tumor volumes covered a wider range, from 33 to 77 mm^3 for Renca, 78 to 132 mm^3 for 786-O and 66 to 130 mm^3 for Caki-1. In these cases, animals were ranked by starting tumor volume, paired from the lowest to the highest volume, and a matched-pair t-test was performed. Survival analysis was performed using the definition of animal death as per animal tumor

models and a test for significance using the log-rank (Mantel-Cox) test. Risk tables are presented in Additional file 2: Appendix B.

Results

IC50 of cell lines treated with iMN013

iMN013 has been tested in numerous cell lines, including those of the NCI60 panel [1]. Because iMN013 undergoes hydrolysis in an aqueous medium, iMN013 half-life was determined in tissue culture medium under standard conditions and found to be 1.5 hours (data not shown). Therefore, the IC50 of selected cell lines was determined after redosing with iMN013 every 12 h (Table 1).

Formulation development

FS-14, an improved derivative of a suspension formulation used in a previously published study [2], was initially used in animal experiments because of its filterability and better injectability. In subsequent experiments this was replaced by FS-19. Pharmacokinetic studies were performed in rats. Three rats were injected SC with 100 µL of 60 mg/mL iMN041 (Table 2). Mean weight of rats injected with FS-14 was 248.7 g, while that of rats injected with FS-19 was 280.7 g.

Screening pharmacokinetics were performed on iMN041 in FS-19 on 3 dogs and demonstrated a half-life of 4.3 hours.

Mouse tumor models

iMN041 was tested in three different tissue types in animal models. In renal cancer, iMN041 was tested in a syngeneic Renca model to determine whether iMN041 upregulated the antitumor immune response in immunocompetent hosts. iMN041 was also tested in xenograft models of human cancer, the TNBC cell line DU4475, ccRCC cell lines 786-O and Caki-1, and pancreatic cancer cell lines CFPAC-1 and SW1990. For the efficacy experiments, iMN041 was administered SC every other day (qod) at the indicated dose for up to 42 days.

Table 2 Pharmacokinetics of iMN013 released from iMN041 formulated in FS-14 or FS-19. Where: Cmax is the maximum concentration, Tmax is the time associated with Cmax, T1/2 is the half-life, MRT is the mean residence time and AUC is the area under the curve

Formulation	Cmax (ng/mL)	Tmax (h)	T1/2 (h)	MRT0-last (h)	AUC0-last (h)
FS-14	1630	0.5	1.02	1.83	3624
FS-19	1770	0.5	1.40	2.27	4815

FACS analysis of tumors in the Renca syngeneic model

When the tumor reached an approximate volume of 270 mm^3, treatment of BALB/c female mice was initiated with 1 mg iMN041 SC qod for two doses or the same volume of PBS (n = 4 per group). This starting tumor volume was necessary to provide sufficient tumor for FACS analysis 4 days after the start of treatment. At that time, tumors were harvested and subjected to FACS analysis (Fig. 1).

The percentage of NK cells positive for granzyme B in the control group was 70.1, which increased to 82.2. in the treated group (p = 0.024), and in NKT cells it increased from 49.9 to 74.2 (p = 0.004) (Fig. 1A-D). An increased ratio of CD8 cytotoxic T-cells to T-regulatory (Treg) cells was noted in treated mice compared to control mice (0.69 to 2.86, p = 0.0026) and CD4 effector to Treg cells (3.70 to 8.74, p = 0.022) (Fig. 1E, F). The percentage of live tumor cells decreased from 47.1 to 32.9 (p = 0.056) (Fig. 1G). The percentage of live cells increased for NK (0.50 to 0.78), NKT (0.062 to 0.085), and CD8-T (0.45 to 0.81), though these differences were not statistically

Table 1 IC50 of iMN013 following a single dose of iMN013 and 72 hour incubation, and following redosing every 12 hours x 6 doses

Cell Line	IC50 of iMN013 (nM)			
	72 h Exposure	72 h Exposure	12 h Redosing	12 h Redosing
EMT-6	1.25	1.58	0.22	0.24
4T1	>100	>100	0.24	0.35
DU4475	3.54	3.73	0.09	0.09
MCF-7	15.2	12.3	0.14	0.12
MDA-MB-231	>100	>100	>100	>100
BxPC-3	44	>100	0.23	0.26
CFPAC-1	3.69	3.52	0.10	0.12
MiaPaca-2	8.48	7.81	0.10	0.10
SW1990	1.68	1.57	<0.1	<0.1
Renca	6.1	7.7	0.48	0.55

significant. The percentage of T-regulatory (Treg) cells decreased in the treated animals from 0.69 to 0.30 (p = 0.071). Lower percentages of myeloid derived suppressor cells (MDSC) were noted in treated vs. control, for PMN-MDSC (polymorphonuclear leukocytes-MDSC) (23.0 to 15.9, p = 0.065) and M-MDSC (monocyte-MDSC) (8.0 to 3.7, p = 0.034) (Fig. 1H, I). MAGE-A expression was analyzed as a marker of iMN041 activity. Live tumor cells in control animals were 91.2% positive for MAGE-A expression compared to 64.2% (p = 0.046) in treated animals (Fig. 1J, K).

Renca syngeneic tumor model of iMN041 efficacy

Renca cells are reported to have cells have one wild type (WT) p53 allele and one allele with the R210C mutation, the effect of which on p53 activity is unclear [4]. As shown in Fig. 2, the tumor volume in the treated mice was significantly smaller than that in the control mice on study days (days) 2-16 (p < 0.01), and the median survival of the treated mice was significantly increased (25 vs. 16 days, p < 0.0001).

Renal cancer xenograft models of iMN041 efficacy

Two different cell lines were implanted into nude mice. The 786-O cell line is a human ccRCC cell line that is Von Hippel Lindau (VHL) defective and p53 mutant. The Caki-1 cell line originates from metastatic ccRCC and is WT VHL and p53 [5, 6]. As in Fig. 3A, mice with 786-O had significantly lower (p < 0.05) tumor volume in treated (0.56 mg qod in FS-14) vs. control animals on days 4-42 (Fig. 3A). In the treated group, one mouse was cured, and no tumor was found by histopathology. No mortality was recorded in iMN041 treated or vehicle control groups.

Mice with Caki-1 implants (Fig. 3B) had significantly lower (p < 0.05) tumor volumes in treated (0.56 mg qod in FS-14) compared to control animals on days 10-35 (Fig. 3B). The study was terminated as per the protocol on day 42; hence, the median survival of treated mice vs. control mice could not be determined (Fig. 3C). Three mice were euthanized for > 20% weight loss in the control group and none in the treated group. These two groups of mice underwent a histologic study to quantitate the amount of tumor necrosis. Necrosis was present in 22.0% of untreated tumor cells vs 9.4% of treated tumor cells (p = 0.021 (see Additional file 1: Appendix A).

As shown in Fig. 3D, mice with Caki-1 implants had signicantly lower tumor volumes noted in treated (0.8 mg qod in FS-19) vs. control animals, (p < 0.05) days 6-42. Mortality was insufficient for the evaluation of survival (death of one mouse in iMN041 treated and vehicle control groups). A comparison was performed on effectiveness of 0.8 mg dose on day 34 vs. 0.56 mg dose on day 35 (day 35 was the last day when all vehicle control mice in the 0.56 mg study were alive). Tumors were rank ordered by starting tumor volume, and then a ratio was calculated for matched pairs of tumor volume from treated animals divided by tumor volume in control animals. A comparison was then performed between the ratios of the two doses. The mean tumor ratio (iMN041/vehicle) in the 0.56 mg study was 0.66 vs. 0.36 in the 0.8 mg study (p = 0.044).

Pancreatic xenograft models of iMN041 efficacy

CFPAC-1 is a p53 mutant human ductal adenocarcinoma cell line [5]. SW1990 is a cell line derived from metastatic pancreatic adenocarcinoma and is variously described as p53 WT [7] or mutant [5].

Tumor volumes in mice treated with iMN041 and implanted with SW1990 were significantly smaller than those in control mice on days 4-36 (p < 0.025) (Fig. 4A). The median survival of treated mice was significantly longer than that of control mice (42 vs. 30 days, p < 0.0001) (Fig. 4B).

Based on a tolerability study in immunocompetent CD-1 male mice (data not shown), mice implanted with CFPAC-1 were started on a dose of 1.2 mg SC qod of iMN041 in FS-19 or PBS (n =10 per group) (see Fig. 4C). Because of toxicity, the dose was reduced to 1 mg SC qod on day 6 and then 0.8 mg SC qod on day 16. Two mice died because of drug toxicity in the treated group (one day 4, the other day 6). The tumor volumes in the treated mice were significantly smaller than those in the control mice on days 2-42 (p < 0.0001). There was insufficient mortality to determine survival rates.

(See figure on next page.)

Fig. 1 Analysis of live cells in mouse Renca tumors. Comparisons of tumors treated with two doses of 1 mg iMN041 SC qod followed by a 48 h observation period or vehicle control (n = 4/group), where * signifies differences where p < 0.05 and ** p < 0.01. **A** Gating strategy for granzyme **B** in NK cells. **B** Gating strategy for granzyme **B** in NKT cells. **C** The percentage of CD45+ cells positive for granzyme **B**. **D** Mean fluorescence intensity (MFI) of CD45+ cells for granzyme **B**. **E** Gating strategy for CD4-T and CD8-T cells. **F** Comparison of CD8-T to Treg percentage cells ratio and CD4-T to Treg percentage cells ratio. **G**, **I** Comparison of live CD45+ cells and live tumor cells, respectively. **H**, **J** Comparison of subsets of CD45+ cells. **K** Gating strategy for detection of MAGE-A expressed by live tumor cells. **L** Positive rate of MAGE-A in tumor cells

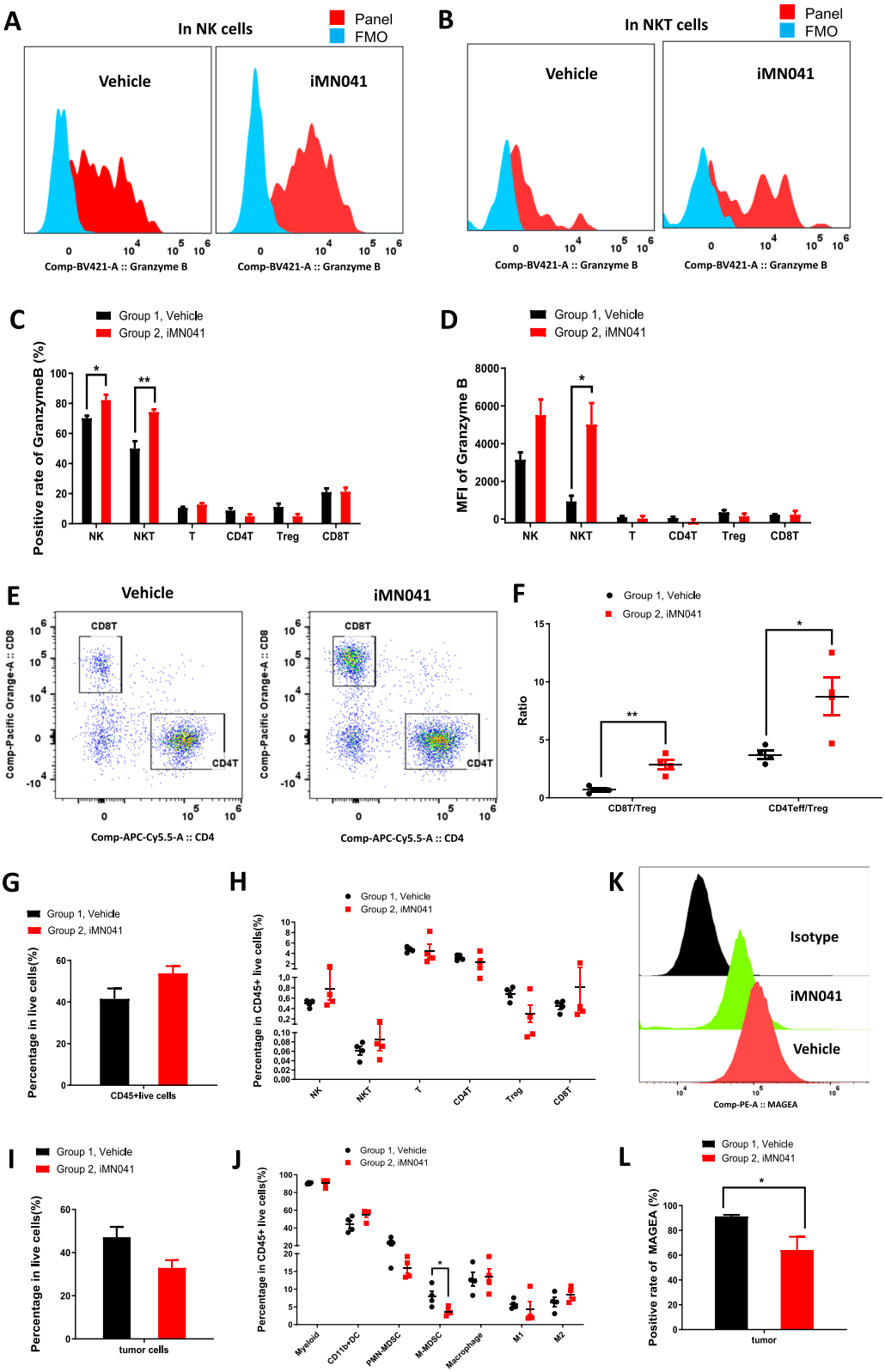

Fig. 1 (See legend on previous page.)

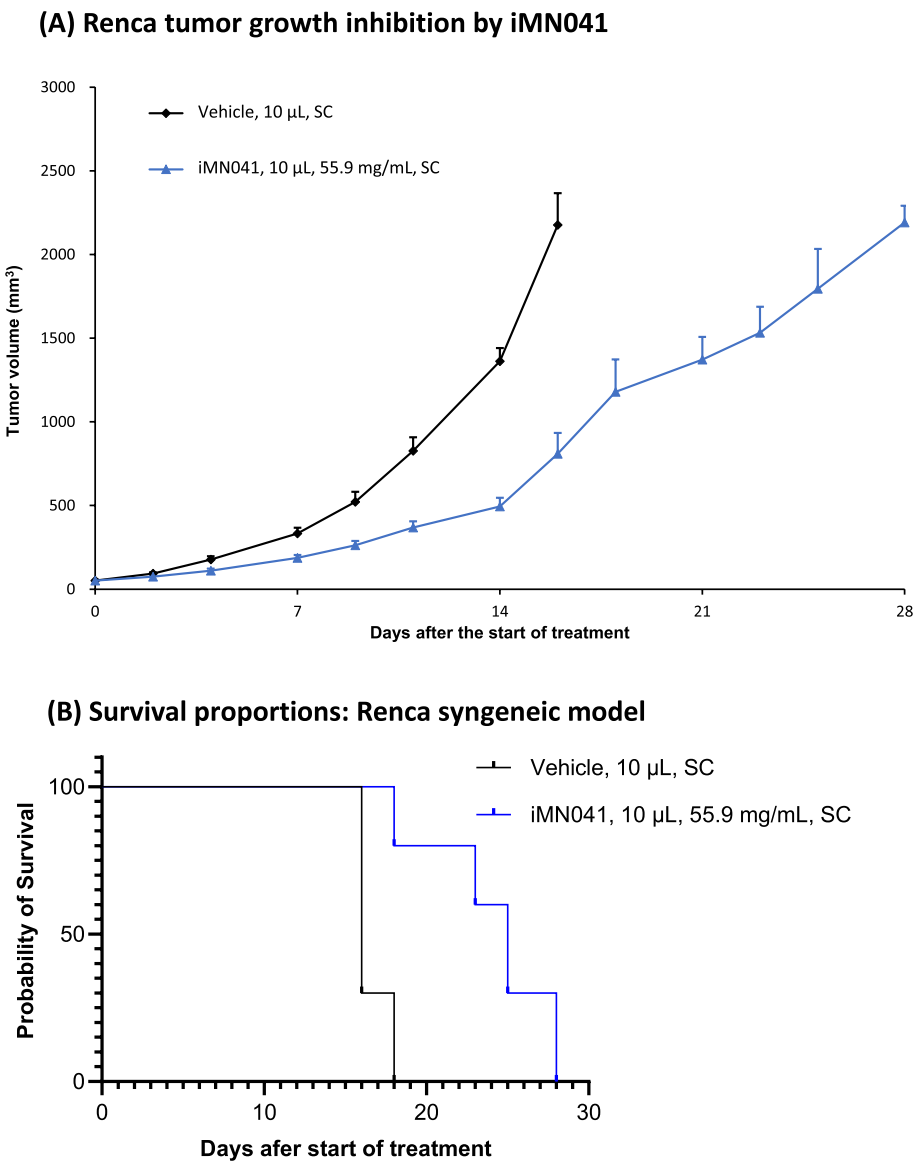

Fig. 2 Mice were administered 0.56 mg iMN041 SC qod in FS-14 or PBS (n = 10 per group). At the start of treatment, mean tumor volume +/- standard deviation (SD) was 52 mm^3 +/- 15.6. **A** Graph of Renca tumor volume in iMN041 treated versus control animals. **B** Survival proportions in treated versus control (25 vs. 16 days, $p < 0.0001$)

Triple negative breast cancer xenograft of iMN041 efficacy

The p53 WT DU4475 cell line was derived from a patient with TNBC [5]. Treated mice implanted with DU4475 were initially administered at two different doses (see Fig. 5A) but mice, particularly in the 0.8 mg group, required dose adjustments (see Materials and Methods); hence, the dose was decreased in both treated groups to 0.5 mg qod on day 8 because of concern that weight loss in the treated and control groups could complicate the assessment of drug toxicity and efficacy. Tumor volume in treated mice was significantly smaller than that of control mice: In the 0.8 mg group, on days 4-20 ($p < 0.05$) and in the 0.6 mg group, on days 4-20 ($p < 0.01$). The median survival of 0.8 mg treated mice vs. control mice was 21 vs. 18 days ($p = 0.019$) and for the 0.6 mg treated mice was 25 vs. 18 days ($p = 0.0032$) (Fig. 5B).

Discussion

iMN013 has been shown to be a DNMTI and an RNRI. Its mechanism of action as a DNMTI and RNRI is identical to that of decitabine and gemcitabine, respectively, although it is much better tolerated than either in mice. There is no evidence that iMN013 is a DNA chain terminator like gemcitabine [8]. iMN013 has been shown to

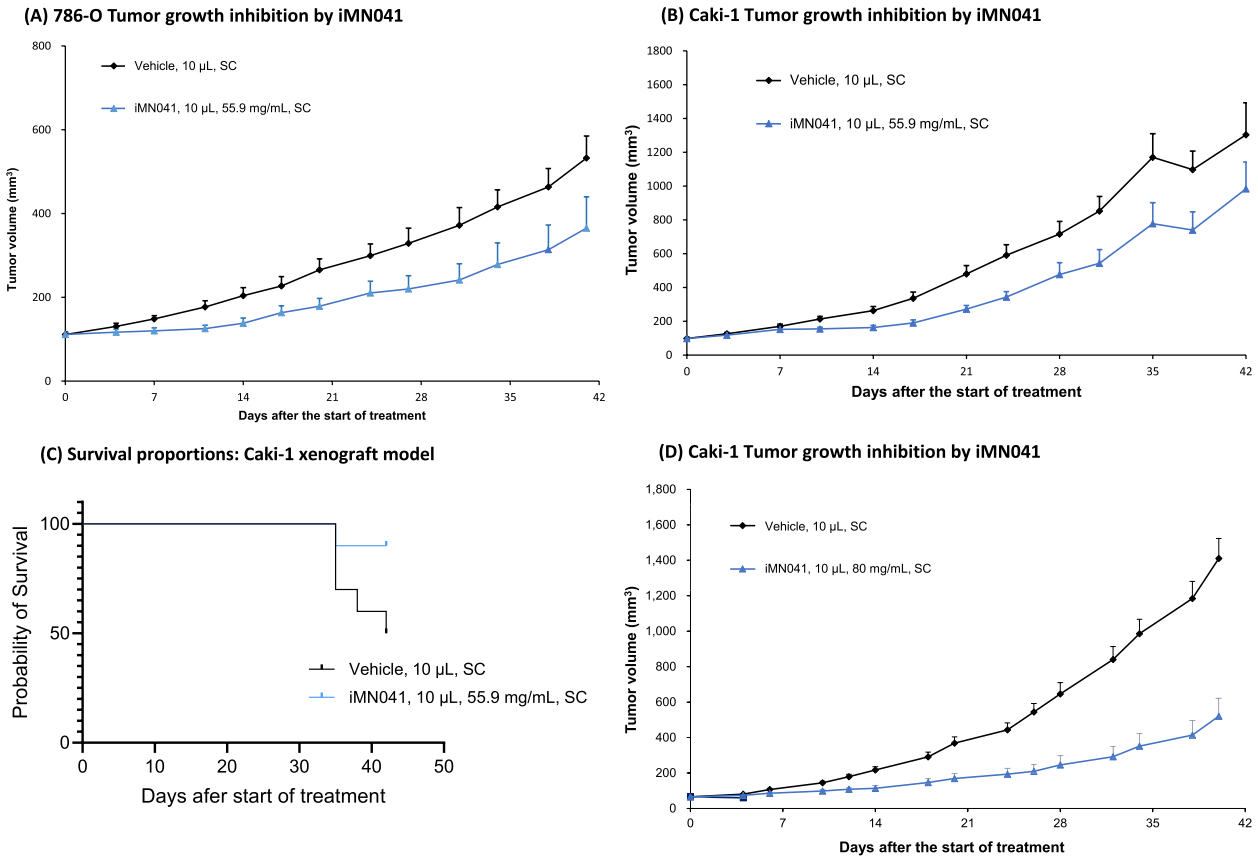

Fig. 3 **A** Mice with 786-O tumors were administered 0.56 mg iMN041 SC in FS-14 qod or PBS (n = 10 per group). Graph of 786-O growth in iMN041 treated versus vehicle control animals. Mean tumor volume +/- SD at study initiation was 111 mm^3 +/- 16.7. **B**, **C** Mice with Caki-1 tumors were administered 0.56 mg iMN041 SC in FS-14 qod or PBS (n = 10 per group). Mean tumor volume +/- SD at study initiation was 98 mm^3 +/- 18.4. **B** Graph of Caki-1 growth in iMN041 treated versus control animals. **C** Survival proportion in Caki-1 implants, treated versus control animals. (> 42 days (undefined) vs. 42 days, p = 0.061). **D** Mice with Caki-1 tumors were administered 0.8 mg iMN041 SC in FS-19 qod or PBS (n = 10 per group). Graph of Caki-1 growth in iMN041 treated versus control animals. Mean tumor volume +/- SD at study initiation was 66 mm^3 +/- 11.5

be particularly effective against cancer cells expressing p53 WT [1]. p53 is often inactivated in cancer because it can trigger cell growth arrest, apoptosis, autophagy or senescence, which are detrimental to cancer cells, and it impedes cell migration, metabolism and angiogenesis, which are favorable for cancer cell progression and metastasis [9]. In addition to TP53, DNMTI upregulate a number of other tumor suppressor genes, including, connexin 32 [10], APAF-1 [11], sFRP2 [12], and HSPB7 in a p53 dependent manner [13]. RCC is strongly associated with loss of VHL expression. Decitabine re-expressed VHL in tissue culture and in a mouse xenograft model [14]. DNMTI have shown potential to affect the immune system through multiple mechanisms, including, upregulation of tumor antigen expression, increased MHC class I expression, and blunting of MDSC expansion [15]. However, it should be noted that the therapeutic efficacy of the current generation DNMTI in solid tumors is not as evident as in hematologic malignancies [16, 17].

iMN013 also inhibits RNR, an enzyme responsible for catalyzing reactions that generate deoxynucleoside triphosphates for DNA synthesis, resulting in reduced deoxynucleotide concentrations. The reduction in the intracellular concentration of endogenous deoxycytidine nucleotides favors the incorporation of iMN013 triphosphate into DNA, a phenomenon described as self-potentiation [1, 18]. The inhibition of RNR by iMN013 leads to enhanced activity against p53 WT tumors by inhibiting p53R2, whereas p53R2 is inducible by decitabine, a mechanism described as self-antagonism [1]. High levels of RNR have been correlated with poor outcomes in a number of cancers, including breast cancer [19] and lung adenocarcinoma [20]. Overexpression of the RRM2 small subunit of RNR creates an immunosuppressive tumor microenvironment. Infiltration of anti-tumor immune cells, such as CD8-T, was significantly lower in the RRM2-high group than in the RRM2-low group, whereas immunosuppressive Treg cells were more

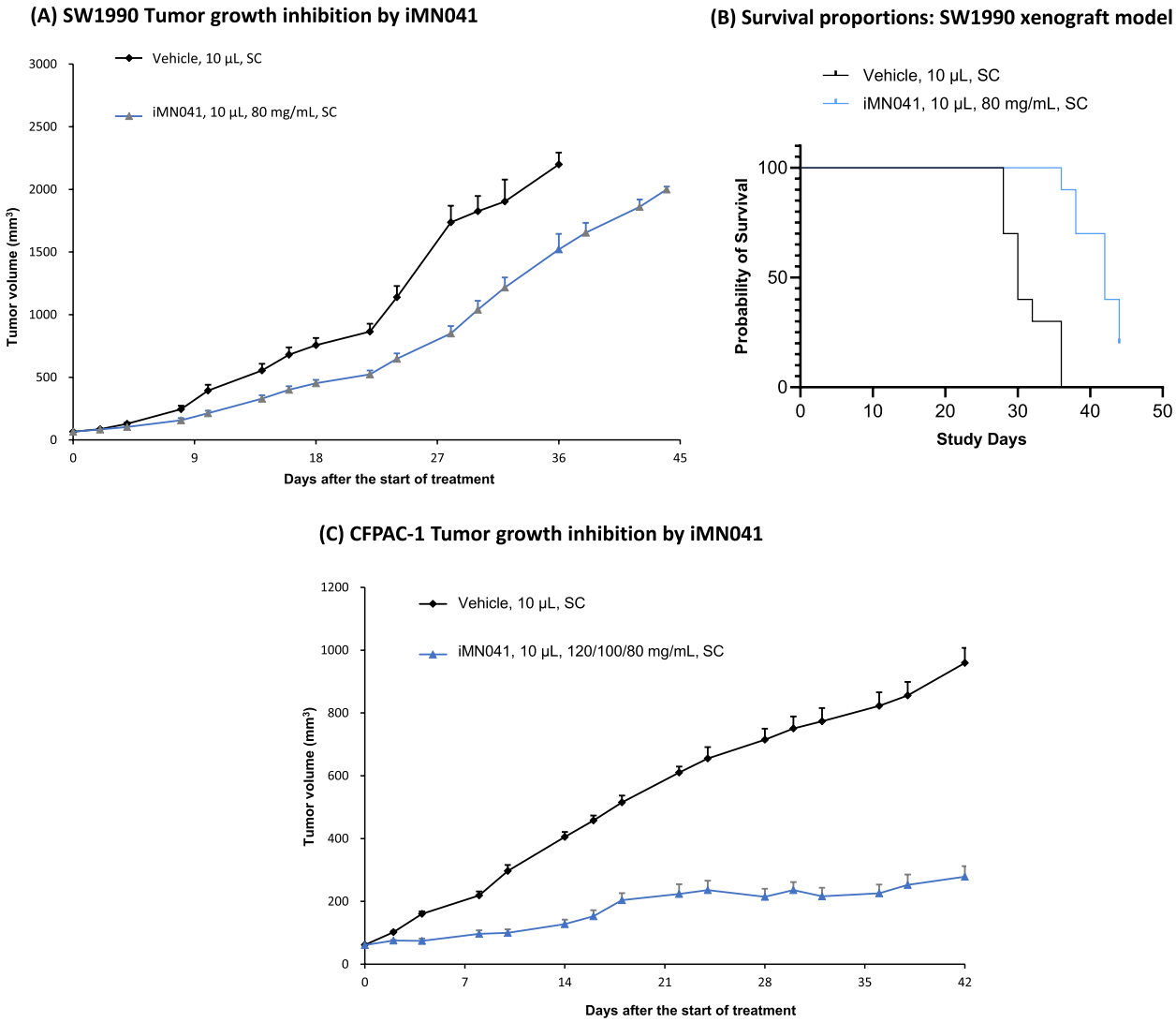

Fig. 4 **A**, **B** Mice with SW1990 tumors were administered 0.8 mg iMN041 SC in FS-19 qod or PBS (n = 10 per group). Mean tumor volume +/- SD at study initiation was 65 mm^3 +/- 6.6. **A** Graph of SW1990 growth in iMN041 treated versus control animals. **B** Survival proportions in SW1990 implants, treated versus control. (42 vs. 30 days, $p < 0.0001$). **C** Mice with CFPAC-1 tumors were initially administered 1.2 mg iMN041 SC in FS-19 qod or PBS (n = 10 per group). Graph of CFPAC-1 growth in iMN041 treated versus vehicle control animals. Mean tumor volume +/- SD at study initiation was 61 mm^3 +/- 5.4

abundant in RRM2-high tumors [21]. Gemcitabine has been shown to decrease Treg cells in patients with pancreatic cancer [22], while decitabine augments the inhibitory effect of Treg cells and restores immune tolerance in several inflammatory diseases [23]. In two solid tumor models, decitabine had no effect or increased Treg cells. In a mouse melanoma model, guadecitabine, a prodrug of decitabine, showed no difference in tumor Treg cells between the treated and control groups [24], and decitabine increased circulating Treg cells in patients with hepatocellular carcinoma and hepatitis B virus [25].

As shown in Table 1, under redosing conditions, the IC_{50} of iMN013 decreased from the micromolar to the nanomolar (nM) range, with three exceptions. 4T1 and BxpC-3, which were resistant to IMN013, demonstrated sensitivity in the nM range, while MDA-MB-231 remained resistant. These data provided further rationale for testing iMN041 in animal models. iMN013/041 has demonstrated activity in mouse models of human leukemia and in breast , colon, lung, pancreatic and renal cancers. The in vitro efficacy of iMN013 in any given cell line has always been translated to its in vivo efficacy,

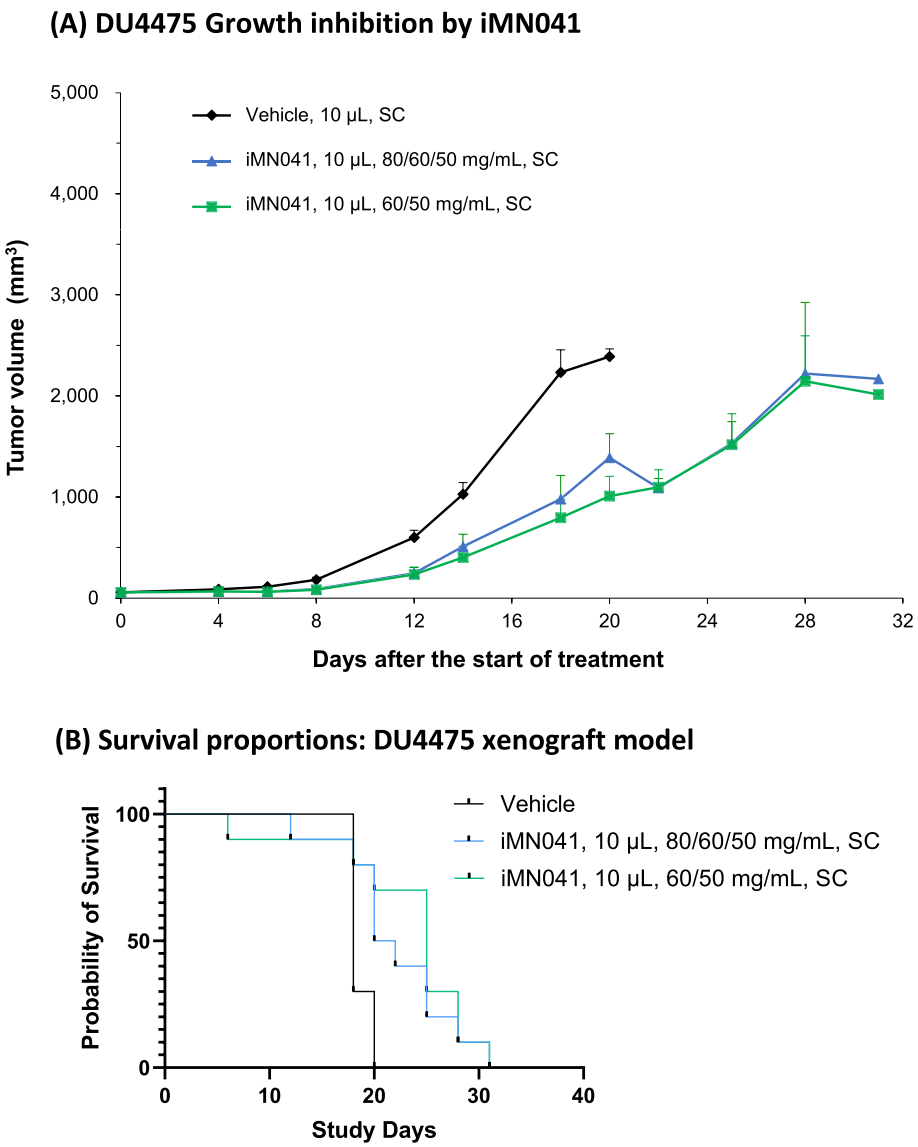

Fig. 5 **A**, **B** Mice with DU4475 tumors were initially administered 0.8 mg or 0.6 mg iMN041 SC in FS-19 qod or PBS (n =10 per group). Mean tumor volume +/- SD at study initiation was 57 mm^3 +/- 7.4. **A** Graph of DU4475 growth in iMN041 treated versus vehicle control animals. **B** Survival proportions in DU4475 implants: 0.8 mg treated mice vs. control mice 21 vs. 18 days (p = 0.019), 0.6 mg treated mice 25 vs. 18 days (p = 0.0032)

suggesting that the treatment of other cancers with iMN041 is possible, such as melanoma or ovarian cancer.

In previous experiments, iMN013 released from iMN041 demonstrated improved pharmacokinetics and pharmacodynamics compared to the administration of iMN013 [2]. Further improvements were necessary for filterability, injectability, pharmacokinetics and tolerability. To this end, experiments were conducted using rats. The FS-19 formulation showed improved pharmacokinetics for iMN013 released from iMN041 for all listed parameters and, most importantly, in AUC over FS-14. FS-19 has also demonstrated better tolerability (data not shown). FS-14 was used to formulate iMN041 in the earlier series of animal models (Renca, 786-O and Caki-1) and iMN041 formulated in FS-19 was administered to animals with Caki-1, CFPAC-1, SW1990, and DU4475 tumors.

Based on the observation of tumor inflammation and ulceration in mice implanted with NCI-H460 cells and treated with iMN041, we hypothesized that the treated nude mice demonstrated enhanced NK cell activity. The purpose of the Renca syngeneic model was to test this hypothesis and observe antitumor immune responses in immunocompetent animals. In this model, iMN041

was shown to (1) significantly increase granzyme B in NK and NKT cells, increasing NK and NKT tumor cell cytotoxicity [26], and (2) significantly increase CD8-T/Treg and CD4-T/Treg, again suggesting its potential to increase the antitumor immune response [27]. Trends in increased numbers of NK, NKT and CD8-T cells and decreased numbers of Treg cells were noted in iMN041 treated animals, consistent with these data. There are no reports in the literature on the increase in the function or proliferation of NKT cells after exposure to DNMTI. An elusive goal of immunotherapy has been to decrease Treg cells while sparing tumor-specific effector T-cells [28], which was the case in this experiment. (3) M-MDSC were significantly decreased with a trend towards a decrease in PMN-MDSC, suggesting a decrease in the likelihood of tumor immune escape [29]. MDSC are generated during tumor progression and suppress antitumor functions of T and NK cells. Their enrichment is associated with poor prognosis of immunotherapy in cancer patients. MDSC also recruit other immunosuppressive cells such as Treg cells. Several therapeutic approaches have been investigated to target MDSC and to overcome their immunosuppression [30].

MAGE-A, (melanoma-associated antigen)-A, is a protein that is not expressed in most normal tissues, except the testis, but is activated in a number of different cancers, including head and neck [31], non-small cell lung cancer [32], melanoma [33], and ovarian [34, 35]. Overexpression of MAGE-A has been associated with a poor prognosis in several cancers [36]. DNMTI have been demonstrated to increase MAGE-A levels in vitro in several tumors, including breast [37], pancreas [38] and colon [39]. Because of this activity, attempts have been made to combine decitabine with dendritic cell vaccination [40] or T-cell therapy [41]. A recent study was reported to be the first to reveal the killing of myelodysplastic syndrome cells by in vitro generated tumor-specific CTLs, after exposure to decitabine [42]. To our knowledge, our study is the first report of a DNMTI decreasing the proportion of cells expressing MAGE-A in vivo, probably as a result of CD8-T cells targeting MAGE-A expressing tumor cells, whereas other DNMTI may decrease CD8-T cells mediated by Treg expansion [43]. This hypothesis is supported by the fact that (1) 91.2% of Renca tumor cells expressed MAGE at baseline and (2) the proportion of decrease in MAGE-A positive cells in iMN041 treated tumors was 29.6% and that of live tumor cells was almost identical at 31.1%.

The xenograft mouse models demonstrated the efficacy of iMN041 with significant inhibition of tumor growth by iMN041 and further improvements with the introduction of the FS-19 formulation, leading to decreased vehicle toxicity and improved pharmacokinetics. Significant inhibition of tumor growth was demonstrated in models of ccRCC (786-O and Caki-1), pancreatic cancer (CFPAC-1 and SW1990) and TNBC (DU4475). Improvements in survival were observed in models with a sufficient number of events during the 42-day study period for all three tissue types. Notably, treatment of mice implanted with DU4475 was particularly difficult because the treated and control mice rapidly started losing weight, making it difficult to determine whether the weight loss was due to the course of the disease or the study drug. This was the rationale for administering a dose of 0.5 mg as opposed to more typically 0.8 mg in animals with other tumor cell lines.

RCC was selected for treatment with iMN041 because in the NCI60 cell panel, five of seven cell lines were sensitive to iMN013 in a conventional assay, with an IC_{50} of less than 10 μM.1 Additionally, RCC is classified as an immunogenic tumor, as is melanoma, because of the occurrence of spontaneous regression, response to immunotherapy and high level of T-cell infiltration [44]. Immune checkpoint inhibitors have become the first-line treatment for metastatic RCC [45]. However, high-dose interleukin-2 (IL-2) is the only systemic therapy associated with durable complete remissions, although only in approximately 5% of patients [46]. IL-2 activates lymphokine activated killer (LAK) cells leading to lysis of tumor cells. LAK cells are mainly composed of NK cells and T-cells [47]. However, the administration of high-dose IL-2 requires hospital admission because patients can experience severe side effects from the treatment [48]. In our study, one mouse implanted with 786-O cells and treated with iMN041 was cured, with no tumor found on histopathology. It is interesting to note that decitabine has been reported to have no activity in a mouse xenograft of 786-O (VHL-defective) [14]. As both iMN013 and decitabine have been reported to cause p53 independent apoptosis at submicromolar doses,1 these results suggest that the difference in activity against 786-O cells may be due to the antitumor immune response induced by iMN041. Treatment of Caki-1 implants with a higher dose of iMN041 that could be administered with FS-19, and the improved pharmacokinetics, translated into improved outcomes over iMN014 formulated in FS-14.

Because of their low mortality, Caki-1 inoculated mice were selected for a substudy to quantitate the amount of necrosis in the tumors. Necrosis was of interest because a study with mice inoculated with NCI-H460 had demonstrated on histology a marked inflammatory response, necrosis and in some cases ulceration [2]. A significant decrease in necrosis was observed in the treated vs. the control group. Tumor necrosis is associated with rapid

tumor growth and is a predictor of poor prognosis in cancer [49, 50].

Pancreatic cancer has a very poor prognosis, and gemcitabine, an RNRI, remains a mainstay of treatment [51]. The main cure for pancreatic cancer is surgical resection and all other treatment modalities have low survival rates. Many clinical trials have assessed the efficacy of immunotherapeutic strategies, however, none has shown dramatic results [52]. In our study, animals with pancreatic cancer demonstrated a good response to treatment, particularly animals implanted with CFPAC-1, when compared to a report in the literature on treatment with gemcitabine in mice with the identical mean starting tumor volume [53].

Breast cancer is categorized into three major subtypes based on the presence or absence of estrogen receptors (ER), progesterone receptors (PR), and human epidermal growth factor 2 (ERBB2, formerly HER2). TNBC lacks all three standard molecular markers (15% of patients) [54]. Most new treatment options for metastatic breast cancer recently approved by the Food and Drug Administration (FDA) are only effective for ER/PR (+) or ERBB2 (+) metastatic tumors, and the subset of patients with metastatic TNBC is treated with chemotherapy alone. Hence, there is a need for novel therapies and immunotherapy may be a viable treatment strategy [55]. DU4475 is a model of aggressive TNBC and there are few reports in the literature of successful treatment of xenografts [56, 57]. Despite issues related to optimal dosing, iMN041 significantly inhibited tumor growth and improved survival.

DNA methyltransferase inhibitors have suffered two main shortcomings that limit their therapeutic use: poor pharmacokinetics and low efficacy in solid tumors [58]. iMN013 is comprised of the sugar of decitabine and the base of gemcitabine, and demonstrates substantially more activity in solid tumors than the current DNMTI, while being less toxic than either [1]. iMN041 has demonstrated promise as an anticancer immunotherapeutic. The derepression of tumor suppressor genes in cancer cells, such as p53, and RNR inhibition, lead to the enhancement of innate and acquired immunity, while decreasing the likelihood of tumor immune escape. It is likely that even better results would have been achieved in tumors in immunocompetent hosts, as nude mice have a vestigial thymus and are incapable of producing mature T-cells [59]. iMN041 has been shown to be effective against decitabine-resistant tumors. One target of iMN041 has been demonstrated to be tumor cells expressing MAGE-A. Although many therapies are under development to target one arm of the antitumor immune response, such as inhibitors of MDSC or Treg cells, iMN013/041 simultaneously affects multiple arms of the immune system. This should simplify patient treatment, minimize the likelihood of tumor escape and improve patient outcomes.

Abbreviation

ACN	Acetonitrile
AUC	Area under the curve
ccRCC	clear cell renal cell carcinoma
Cmax	Maximum drug concentration
DNMTI	DNA methyltransferase inhibitor
ER	Estrogen receptor
ERBB2	Human epidermal growth factor 2
FACS	Fluorescent activated cell sorting
FBS	Fetal bovine serum
FMO	Fluorescein minus one
h	hours
IC_{50}	Half-maximal inhibitory concentration
IL-2	Interleukin-2
LC/MS	Liquid chromatography/mass spectrometry,
MAGE	Melanoma associated antigen
MDSC	Myeloid derived suppressor cells
MRT	Mean residence time
NK	Natural killer cells
PBS	Phosphate buffered saline
PK	Pharmacokinetic
PR	Progesterone receptor
qod	Every other day
RNRI	Ribonucleotide reductase inhibitor
RRM2	Small subunit 2 of RNR
SC	Subcutaneous
Tmax	Time associated with Cmax
TNBC	Triple negative breast cancer
Treg	T regulatory cells
$T_{1/2}$	Drug half-life
VHL	Von Hippel Lindau
WT	Wild type

Supplementary Information

The online version contains supplementary material available at https://doi.org/10.1186/s41231-024-00161-3.

Additional file 1: Appendix A. Histopathology of renal cell cancer Caki-1 tumors and quantitation of tumor necrosis. **Table 1.** Calculation of percentage necrosis from representative tumor from mice inoculated with Caki-1 at end of study. Mice 1-2 through 2-5 were treated with vehicle (PBS), while mice 3-1 through 4-5 were treated with 0.56 mg iMN041 SC in FS-14 qod for up to 42 days. **Figure 1.** Representative images of tumors from vehicle control mice inoculated with Caki-1 cells at end of study. Hematoxylin and eosin (H&E) staining at 200X. **Figure 2.** Representative images of tumors from iMN041 treated mice inoculated with Caki-1 cells at end of study. Hematoxylin and eosin (H&E) staining at 200X.

Additional file 2: Appendix B. Risk tables. Risk tables for survival graphs presented in the text. Where 1-1 to 2-5 identify mice administered vehicle (PBS) and 3-1 to 4-5, and where appropriate 5-1 to 6-5, identify iMN041 treated mice. Dosing is specified in the text. Study Days refer to number of days from start of treatment to event or censoring. Under Group A or B heading, (1) refers to event, as define in Statistical analysis, and (0) to censoring. **Table 1.** Risk table for Renca. **Table 2.** Risk table for Caki-1. **Table 3.** Risk table for SW1990. **Table 4.** Risk table for DU4475.

Acknowledgements
None.

Authors' contributions
RD designed the studies, analyzed and interpreted and data, and wrote the manuscript. YZ, JW, and QG provided the methodology to conduct the studies. All authors read and approved the final manuscript.

Funding
This study was funded by Epigenetics Pharma.

Availability of data and materials
The data generated in this study are available upon reasonable request from the corresponding author.

Declarations

Ethics approval and consent to participate
All animal studies were conducted under the animal-use protocol and animal welfare policy of WuXi App Tec.

Consent for publication
Not applicable.

Competing interests
RD is the inventor of iMN013 and iMN041 and majority shareholder of Epigenetics Pharma.

Author details
[1]Epigenetics Pharma, 244 Davison Head Dr, Friday Harbor, WA 98250, USA.
[2]Oncology and immunology, WuXi App Tec, Shanghai 200131, China.

Received: 13 October 2023 Accepted: 4 January 2024
Published online: 19 January 2024

References

1. Daifuku R, Hu Z, Saunthararajah Y. 5-aza-2′,2′-Difluoro Deoxycytidine (NUC013): A Novel Nucleoside DNA Methyl Transferase Inhibitor and Ribonucleotide Reductase Inhibitor for the Treatment of Cancer. Pharmaceuticals (Basel). 2017;10(3):65.
2. Daifuku R, Grimes S, Stackhouse M. NUC041, a Prodrug of the DNA Methytransferase Inhibitor 5-aza-2′,2′-Difluorodeoxycytidine (NUC013), Leads to Tumor Regression in a Model of Non-Small Cell Lung Cancer. Pharmaceuticals (Basel). 2018;11(2):36.
3. Hather G, Liu R, Bandi S, Mettetal J, Manfredi M, Shyu WC, et al. Growth rate analysis and efficient experimental design for tumor xenograft studies. Cancer Inform. 2014;13(Suppl 4):65–72.
4. Kiweler N, Wünsch D, Wirth M, Mahendrarajah N, Schneider G, Stauber RH, et al. Histone deacetylase inhibitors dysregulate DNA repair proteins and antagonize metastasis-associated processes. J Cancer Res Clin Oncol. 2020;146(2):343–56.
5. The TP53 database. [Cited 2023, March 17]. Available from: https://tp53.isb-cgc.org/view_data?bq_view_name=CellLineDownload.
6. Brodaczewska KK, Szczylik C, Fiedorowicz M, Porta C, Czarnecka AM. Choosing the right cell line for renal cell cancer research. Mol Cancer. 2016;15(1):83.
7. ATCC. Pancreatic cancer p53 hotspot mutation cell panel. [Cited 2023, March 17]. Available from: https://www.atcc.org/products/cells_and_microorganisms/cell_lines/human/tumor_cell_panels/panels_by_tissue_type/pancreatic_cancer_cell_panel/tcp-2060.
8. Daifuku R. Pharmacoepigenetics of nucleoside DNA methyltransferase inhibitors. In: Cacabellos R, editor. Pharmacoepigenetics (2nd ed.). Elsevier. 2024: In press.
9. Liu Y, Wang X, Wang G, Yang Y, Yuan Y, Ouyang L. The past, present and future of potential small-molecule drugs targeting p53-MDM2/MDMX for cancer therapy. Eur J Med Chem. 2019;15(176):92–104.
10. Hagiwara H, Sato H, Ohde Y, Takano Y, Seki T, Ariga T, et al. 5-Aza-2′-deoxycytidine suppresses human renal carcinoma cell growth in a xenograft model via up-regulation of the connexin 32 gene. Br J Pharmacol. 2008;153(7):1373–81.
11. Zhu X, Yi F, Chen P, Chen L, Zhang X, Cao C, et al. 5-Aza-2′-Deoxycytidine and CDDP Synergistically Induce Apoptosis in Renal Carcinoma Cells via Enhancing the APAF-1 Activity. Clin Lab. 2015;61(12):1821–30.
12. Konac E, Varol N, Yilmaz A, Menevse S, Sozen S. DNA methyltransferase inhibitor-mediated apoptosis in the Wnt/β-catenin signal pathway in a renal cell carcinoma cell line. Exp Biol Med (Maywood). 2013;238(9):1009–16.
13. Lin J, Deng Z, Tanikawa C, Shuin T, Miki T, Matsuda K, et al. Downregulation of the tumor suppressor HSPB7, involved in the p53 pathway, in renal cell carcinoma by hypermethylation. Int J Oncol. 2014;44(5):1490–8.
14. Alleman WG, Tabios RL, Chandramouli GV, Aprelikova ON, Torres-Cabala C, Mendoza A, et al. The in vitro and in vivo effects of re-expressing methylated von Hippel-Lindau tumor suppressor gene in clear cell renal carcinoma with 5-aza-2′-deoxycytidine. Clin Cancer Res. 2004;10(20):7011–21.
15. Terracina KP, Graham LJ, Payne KK, Manjili MH, Baek A, Damle SR, et al. DNA methyltransferase inhibition increases efficacy of adoptive cellular immunotherapy of murine breast cancer. Cancer Immunol Immunother. 2016;65(9):1061–73.
16. Linnekamp JF, Butter R, Spijker R, Medema JP, van Laarhoven HWM. Clinical and biological effects of demethylating agents on solid tumours - A systematic review. Cancer Treat Rev. 2017;54:10–23.
17. Mehdipour P, Chen R, De Carvalho DD. The next generation of DNMT inhibitors. Nat Cancer. 2021;2(10):1000–1.
18. Drugs.com. Gemcitabine prescribing information. [Cited 2023, March 17]. Available from: https://www.drugs.com/pro/gemcitabine.html#s-34090-1.
19. Zhang H, Liu X, Warden CD, Huang Y, Loera S, Xue L, et al. Prognostic and therapeutic significance of ribonucleotide reductase small subunit M2 in estrogen-negative breast cancers. BMC Cancer. 2014;11(14):664.
20. Ma C, Luo H, Cao J, Gao C, Fa X, Wang G. Independent prognostic implications of RRM2 in lung adenocarcinoma. J Cancer. 2020;11(23):7009–22.
21. Mazzu YZ, Armenia J, Nandakumar S, Chakraborty G, Yoshikawa Y, Jehane LE, et al. Ribonucleotide reductase small subunit M2 is a master driver of aggressive prostate cancer. Mol Oncol. 2020;14(8):1881–97.
22. Eriksson E, Wenthe J, Irenaeus S, Loskog A, Ullenhag G. Gemcitabine reduces MDSCs, tregs and TGFβ-1 while restoring the teff/treg ratio in patients with pancreatic cancer. J Transl Med. 2016;14(1):282.
23. Landman S, van der Horst C, van Erp PEJ, et al. Immune responses to azacytidine in animal models of inflammatory disorders: a systematic review. J Transl Med. 2021;19:11.
24. Amaro A, Reggiani F, Fenoglio D, Gangemi R, Tosi A, Parodi A et al. Guadecitabine increases response to combined anti-CTLA-4 and anti-PD-1 treatment in mouse melanoma in vivo by controlling T-cells, myeloid derived suppressor and NK cells. J Exp Clin Cancer Res. 2023;42(1):67.
25. Fang Y, Yuan XD, Liu HH, Xiang L, Chen LM, Fan YC, et al. 5-Aza-2′-deoxycytidine may enhance the frequency of T regulatory cells from $CD4^+$ naïve T cells isolated from the peripheral blood of patients with chronic HBV infection. Expert Rev Clin Immunol. 2021;17(2):177–85.
26. Rousalova I, Krepela E. Granzyme B-induced apoptosis in cancer cells and its regulation (review). Int J Oncol. 2010;37(6):1361–78.
27. Raskov H, Orhan A, Christensen JP, Gögenur I. Cytotoxic $CD8^+$ T cells in cancer and cancer immunotherapy. Br J Cancer. 2021;124(2):359–67.
28. Ellis GI, Riley JL. How to kill T_{reg} cells for immunotherapy. Nat Cancer. 2020;1(12):1134–5.
29. Ostrand-Rosenberg S, Fenselau C. Myeloid-Derived Suppressor Cells: Immune-Suppressive Cells That Impair Antitumor Immunity and Are Sculpted by Their Environment. J Immunol. 2018;200(2):422–31.
30. Fleming V, Hu X, Weber R, Nagibin V, Groth C, Altevogt P, et al. Targeting Myeloid-Derived Suppressor Cells to Bypass Tumor-Induced Immunosuppression. Front Immunol. 2018;2(9):398.
31. Laban S, Giebel G, Klümper N, Schröck A, Doescher J, Spagnoli G, et al. MAGE expression in head and neck SCuamous cell carcinoma primary tumors, lymph node metastases and respective recurrences-implications for immunotherapy. Oncotarget. 2017;8(9):14719–35.
32. Ayyoub M, Memeo L, Alvarez-Fernández E, Colarossi C, Costanzo R, Aiello E, et al. Assessment of MAGE-A expression in resected non-small cell lung cancer in relation to clinicopathologic features and mutational status of EGFR and KRAS. Cancer Immunol Res. 2014;2(10):943–8.
33. Jungbluth AA, Busam KJ, Kolb D, Iversen K, Coplan K, Chen YT, et al. Expression of MAGE-antigens in normal tissues and cancer. Int J Cancer. 2000;85(4):460–5.
34. Xu Y, Wang C, Zhang Y, Jia L, Huang J. Overexpression of MAGE-A9 Is Predictive of Poor Prognosis in Epithelial Ovarian Cancer. Sci Rep. 2015;15(5):12104.
35. Srivastava P, Paluch BE, Matsuzaki J, James SR, Collamat-Lai G, Taverna P, et al. Immunomodulatory action of the DNA methyltransferase inhibitor

SGI-110 in epithelial ovarian cancer cells and xenografts. Epigenetics. 2015;10(3):237–46.
36. Chen X, Wang L, Liu J, Huang L, Yang L, Gao Q, et al. Expression and prognostic relevance of MAGE-A3 and MAGE-C2 in non-small cell lung cancer. Oncol Lett. 2017;13(3):1609–18.
37. Hou SY, Sang MX, Geng CZ, Liu WH, Lü WH, Xu YY, et al. Expressions of MAGE-A9 and MAGE-A11 in breast cancer and their expression mechanism. Arch Med Res. 2014;45(1):44–51.
38. Bert T, Lubomierski N, Gangsauge S, Münch K, Printz H, Prasnikar N, et al. Expression spectrum and methylation-dependent regulation of melanoma antigen-encoding gene family members in pancreatic cancer cells. Pancreatology. 2002;2(2):146–54.
39. Kim KH, Choi JS, Kim IJ, Ku JL, Park JG. Promoter hypomethylation and reactivation of MAGE-A1 and MAGE-A3 genes in colorectal cancer cell lines and cancer tissues. World J Gastroenterol. 2006;12(35):5651–7.
40. Krishnadas DK, Shusterman S, Bai F, Diller L, Sullivan JE, Cheerva AC, et al. A phase I trial combining decitabine/dendritic cell vaccine targeting MAGE-A1, MAGE-A3 and NY-ESO-1 for children with relapsed or therapy-refractory neuroblastoma and sarcoma. Cancer Immunol Immunother. 2015;64(10):1251–60.
41. Shi X, Chen X, Fang B, Ping Y, Qin G, Yue D, et al. Decitabine enhances tumor recognition by T cells through upregulating the MAGE-A3 expression in esophageal carcinoma. Biomed Pharmacother. 2019;112:108632.
42. Zhang Z, He Q, Tao Y, Guo J, Xu F, Wu LY, et al. Decitabine treatment sensitizes tumor cells to T-cell-mediated cytotoxicity in patients with myelodysplastic syndromes. Am J Transl Res. 2017;9(2):454–65.
43. Stübig T, Badbaran A, Luetkens T, Hildebrandt Y, Atanackovic D, Binder TM, et al. 5-azacytidine promotes an inhibitory T-cell phenotype and impairs immune mediated antileukemic activity. Mediators Inflamm. 2014;2014:418292.
44. Itsumi M, Tatsugami K. Immunotherapy for renal cell carcinoma. Clin Dev Immunol. 2010;2010:284581.
45. Angulo JC, Shapiro O. The Changing Therapeutic Landscape of Metastatic Renal Cancer. Cancers (Basel). 2019;11(9):1227.
46. PDQ Adult Treatment Editorial Board. Renal cell cancer treatment (PDQ®): Health professional version. [Cited 2023, March 17]. Available from: https://www.ncbi.nlm.nih.gov/books/NBK65815/#CDR0000062894__1.
47. Wendel P, Reindl LM, Bexte T, Künnemeyer L, Särchen V, Albinger N, et al. Arming Immune Cells for Battle: A Brief Journey through the Advancements of T and NK Cell Immunotherapy. Cancers (Basel). 2021;13(6):1481.
48. Amin A, White RL. Interleukin-2 in Renal Cell Carcinoma: A Has-Been or a Still-Viable Option? J Kidney Cancer VHL. 2014;1(7):74–83.
49. Yee PP, Li W. Tumor necrosis: A synergistic consequence of metabolic stress and inflammation. Bioessays. 2021;43(7):e2100029.
50. Liu ZG, Jiao D. Necroptosis, tumor necrosis and tumorigenesis. Cell Stress. 2019;4(1):1–8.
51. Huang JH, Guo W, Liu Z. Discussion on gemcitabine combined with targeted drugs in the treatment of pancreatic cancer. World J Gastroenterol. 2023;29(3):579–81.
52. Schizas D, Charalampakis N, Kole C, Economopoulou P, Koustas E, Gkotsis E, et al. Immunotherapy for pancreatic cancer: A 2020 update. Cancer Treat Rev. 2020;86:102016.
53. Li Z, Zou X, Zhu H, Chen M, Zhao Y. Inhibitory effect of baicalein combined with gemcitabine in human pancreatic cancer cell lines. Oncol Lett. 2018;15(4):5459–64.
54. Waks AG, Winer EP. Breast Cancer Treatment: A Review. JAMA. 2019;321(3):288–300.
55. Emens LA. Immunotherapy in Triple-Negative Breast Cancer. Cancer J. 2021;27(1):59–66.
56. Bush TL, Payton M, Heller S, Chung G, Hanestad K, et al. AMG 900, a small-molecule inhibitor of aurora kinases, potentiates the activity of microtubule-targeting agents in human metastatic breast cancer models. Mol Cancer Ther. 2013;12(11):2356–66.
57. Yao HP, Zhuang CM, Zhou YQ, Zeng JY, Zhang RW, et al. Oncogenic variant RON160 expression in breast cancer and its potential as a therapeutic target by small molecule tyrosine kinase inhibitor. Curr Cancer Drug Targets. 2013;13(6):686–97.
58. Mehdipour P, Chen R, De Carvalho DD. The next generation of DNMT inhibitors. Nat Cancer. 2021;2(10):1000–1.
59. Chen J, Liao S, Xiao Z, Pan Q, Wang X, Shen K, et al. The development and improvement of immunodeficient mice and humanized immune system mouse models. Front Immunol. 2022;19(13):1007579.

Publisher's Note